Original Article

Quantitative iTRAQ proteomics reveal the proteome profiles of bone marrow mesenchymal stem cells after cocultures with Schwann cells *in vitro*

Han Ding[1#], Ang Li[1,2#], Chao Sun[1#], Jianping Zhang[1], Jun Shang[1], Haoshuai Tang[1], Junjin Li[1], Min Wang[3], Xiaohong Kong[4], Zhijian Wei[1], Shiqing Feng[1]

[1]International Science and Technology Cooperation Base of Spinal Cord Injury, Tianjin Key Laboratory of Spine and Spinal Cord Injury, Department of Orthopedics, Tianjin Medical University General Hospital, Tianjin, China; [2]Department of Orthopedics, Henan Provincial People's Hospital, People's Hospital of Zhengzhou University, Zhengzhou, China; [3]Tianjin Key Laboratory of Lung Cancer Metastasis and the Tumor Microenvironment, Tianjin Lung Cancer Institute, Tianjin Medical University General Hospital, Tianjin, China; [4]School of Medicine, Nankai University, Tianjin, China

Contributions: (I) Conception and design: H Ding; (II) Administrative support: S Feng; (III) Provision of study materials or patients: A Li; (IV) Collection and assembly of data: C Sun; (V) Data analysis and interpretation: H Ding, Z Wei; (VI) Manuscript writing: All authors; (VII) Final approval of manuscript: All authors.

[#]These authors contributed equally to this work.

Correspondence to: Shiqing Feng, PhD; Zhijian Wei, PhD. Department of Orthopedics, Tianjin Medical University General Hospital, 154 Anshan Road, Heping District, Tianjin 300052, China. Email: sqfeng@tmu.edu.cn; weizhijian2002@126.com.

Background: Bone marrow mesenchymal stem cells (BMSCs) combined with Schwann cells (SCs) represent a better therapeutic cell transplantation strategy for treating spinal cord injury (SCI) than transplantation with BMSCs or SCs alone. In previous studies, we demonstrated that BMSCs are able to differentiate in neuron-like cells when cocultured with SCs. The detailed mechanism underlying SCI repair that occurs during the combined transplantation of BMSCs and SCs has not yet been studied. In this study, we adopted an isobaric tag for relative and absolute quantitation (iTRAQ)-based protein identification/quantification approach to examine the effects of the SC and BMSC coculture process on the BMSCs and then obtained and analyzed the differentially expressed proteins (DEPs) and their possible related pathways.

Methods: This study included three groups based on the number of coculture days (i.e., 0, 3, and 7 days). Changes in BMSC protein expression levels were measured using the iTRAQ technique. A bioinformatics analysis of all the data was performed.

Results: In total, 6,760 types of proteins were detected, corresponding to 5,181 data points with quantitative information. Of these, a total of 243 DEPs were identified, of which 169 proteins were upregulated and 74 proteins were downregulated. These DEPs were identified by Gene Ontology (GO) and Kyoto Encyclopedia of Genes and Genomes (KEGG) analyses. Intercellular adhesion molecule-1 (ICAM-1), integrin, and dioxygenase may play crucial roles in the repair of SCI. The data analysis indicates that the relevant biological processes may be regulated by lysosome function, cell adhesion molecules (CAMs), leukocyte transendothelial migration, and the phosphatidylinositol-3-kinase (PI3K) and peroxisome proliferator-activated receptor (PPAR) signaling pathways.

Conclusions: The data provided in this study indicate that several molecular mechanisms and signaling pathways are involved in the BMSC and SC coculture process. This information may be useful for the further identification of specific targets and related mechanisms and guide new directions for SCI treatment.

Keywords: Proteomics analysis; spinal cord injury (SCI); Schwann cells (SCs); bone marrow mesenchymal stem cells (BMSCs); isobaric tag for relative and absolute quantitation (iTRAQ)

Submitted May 20, 2022. Accepted for publication Jul 05, 2022.
doi: 10.21037/atm-22-3073
View this article at: https://dx.doi.org/10.21037/atm-22-3073

Introduction

Spinal cord injury (SCI) has limited treatment options, and is characterized by high morbidity and disability (1). Currently, no effective treatment method is available for SCI (2). SCI can be divided into primary and secondary injuries based on pathology. A secondary injury comprises a series of complex reactions involving factors, such as free radicals, calcium-ion influx, and macrophage polarization, which can contribute to more severe damage (3-8). Later, glial scar formation and an imbalance in the microenvironment may also prevent the repair of the injured spinal cord. Various therapeutic methods, including cell graft therapy, have been applied to improve functional recovery after SCI. The administration of methylprednisolone, which was once the only Food and Drug Administration-approved drug for the treatment of traumatic acute SCI, has dramatically decreased in many regions, however, some clinicians still believe in its efficacy (9-13).

The transplantation of stem cells provides a potential method to replace injured cells at lesion sites for the repair of SCI, and bone marrow mesenchymal stem cells (BMSCs) are one of the most studied cell types (14-16). BMSCs facilitate the healing of ischemic tissue-related diseases through proangiogenic secretory proteins (17). BMSCs have several beneficial properties, including low immunogenicity, the secretion of a variety of growth factors, and pluripotency, which enable the formation of different phenotypes in response to changes in elasticity at the tissue level (18,19).

Schwann cells (SCs) play significant roles in peripheral nerve injury, a process that is related to different types of macrophages (20). Our previous research revealed that the transplantation of SCs, which is an effective therapeutic method, promotes axonal regeneration and functional recovery after SCI in rats, but the mechanism by which this occurs remains unclear (21-24). We also found that co-transplanting BMSCs with SCs better promotes functional recovery in rats after SCI (23). To explore the potential mechanism underlying the interaction between these two types of cells, we used isobaric tag for relative and absolute quantitation (iTRAQ) to detect differentially expressed proteins (DEPs) in BMSCs cocultured with SCs. iTRAQ analyses on SCI are mainly related to pathological mechanism. However, this study is a continuation of our previous studies just as mentioned. We aim to investigate the potential repair mechanism of co-transplantation BMSCs with SCs which is first reported. We present the following article in accordance with the ARRIVE reporting checklist (available at https://atm.amegroups.com/article/view/10.21037/atm-22-3073/rc).

Methods

Animals

Adult female Wistar rats (Pasteur Institute, China) weighing 180–200 g (n=20) was used in this study. All the procedures in this study, including the use of animals, were approved by the Tianjin Medical University Ethical Committee (No. TMUAMEC2017025) and were conducted in accordance with the Guide for the Care and Use of Laboratory Animals (NIH Publications, revised 2011). The animals were randomly used for the BMSC and SC cultures. A protocol was prepared without registration before the study.

BMSC and SC cultures

The methods used for the BMSC and SC primary cultures were performed as previously described (23,25) with some modifications. Briefly, the rats were anesthetized with 3% pentobarbital sodium (45 mg/kg intraperitoneally) and sacrificed by cervical dislocation. The bilateral sciatic nerve was exposed, and 20 mm of the distal segment of the nerve was resected and placed in a dish containing phosphate buffered solution (Sigma, Germany). After the connective tissue and epineurium were cautiously pulled away with fine forceps under sterile conditions, the remaining nerves were teased apart with a needle and cut into fragments of 2 to 3 mm. The disentangled nerve fragments were digested in a 15-mL sterilized tube containing 0.3% collagenase type II (Invitrogen, USA) at 37 ℃ for 30 minutes with agitation. After the collagenase was removed carefully, the sample was incubated with 0.25% trypsin-ethylenediaminetetraacetic acid (EDTA; Gibco, USA) for 5 minutes in a 37 ℃

incubator. At the same time, both the bilateral femurs and tibias were removed under sterile conditions. The epiphyses were removed and the bone marrow was flushed with Dulbecco's modified Eagle's medium/nutrient mixture F12 (1:1 D/F12, Gibco, USA). The resulting bone marrow fluid was filtered through a 70-μm nylon mesh. Both the SCs and BMSCs were cultured in 75-cm^2 flasks using D/F12 supplemented with 10% fetal bovine serum (Gibco, USA) and 100 U/mL of penicillin and streptomycin (Gibco, USA) at 37 ℃ in a 5% carbon dioxide incubator (ThermoFisher, USA). For the SCs, the basic medium was replaced with a purification medium [a basic medium containing 10 μM of cytosine β-D-arabinofuranoside (Sigma, Germany)] to eliminate the fibroblasts. The purification medium was changed to growth medium [a basic medium containing 20 ng/mL of heregulin 1-β1 (HRG1-β1) extracellular domain (ECD) (R&D systems, USA)] 24 hours later. The medium was changed and replaced every 2–3 days with fresh complete culture medium. The BMSCs and SCs were used for experiments at passages 3–5.

Coculture system for BMSCs and SCs

In the present study, a semi-quantitative medium exchange method was used to coculture the BMSCs and SCs as previously described (23). Briefly, the BMSC medium was completely replaced with 5 mL of BMSC medium and 5 mL of refresh medium. Both cocultures and control cultures were incubated for 3 and 7 days. The following three groups were created and had various coculture durations: Group 1: the BMSCs were cocultured with SCs for 7 days (the SC7d group); Group 2: the BMSCs were cocultured with SCs for 3 days (the SC3d group); and Group 3: the BMSCs were cultured alone (the SC0d group, which served as the control group). Additionally, three replicates with independent samples were used to ensure the reproducibility of the results.

iTRAQ sample preparation

The cell precipitates were homogenized on ice, and 300 mg of homogenate from each group was used for the proteomic screening (26). All the cell samples were lysed with a mixture of 8 M of urea, 50 mM of Tris (pH 8.0), 1% Nonidet P-40 (NP-40), 1% sodium deoxycholate, 1% protease inhibitor, 2 mM of EDTA and 10 mM of dithiothreitol (DTT). A two-dimensional Quant kit (GE Healthcare, USA) was used to establish the protein concentrations. After digestion overnight at 37 ℃ with trypsin (50 μg/mL), the protein samples (250 mg) were labeled with the iTRAQ reagents (5-plex; AB SCIEX, MA, USA) in accordance with the manufacturer's protocol.

Data analysis and bioinformatics

Using the software Protect Discoverer version 1.2, the raw data files acquired from the Orbitrap were converted into a Mascot input file (MGF files) that contained secondary spectrum information. The MGF files were then imported into Mascot software version 2.3 for qualitative and quantitative calculations. The qualitative and quantitative protein information was exported to a comma-separated values file containing all the information for the subsequent analysis. To detect the biological and functional characteristics of all the DEPs, the Gene Ontology (GO) database was used to map the sequences. To identify candidate biomarkers in this process, a pathway analysis was conducted using the Kyoto Encyclopedia of Genes and Genomes (KEGG) database. The protein-protein interaction (PPI) network was analyzed using the Search Tool for the Retrieval of Interacting Genes (STRING) database.

Immunofluorescence staining

The cells were fixed on ice with 4% paraformaldehyde for 15 min. All the staining procedures were performed as previously described (23). Primary antibody S100 (Abcam, USA; ab52642) was diluted in 0.25% Triton X-100 at 1:200. Secondary antibody goat anti-rabbit Alexa Fluor 488 (Abcam, USA; ab150077) was diluted in 0.25% Triton X-100 at 1:500. Images were taken with a fluorescent microscope.

Multilineage differentiation of BMSCs

BMSCs at passage 3 were seed with a concentration of 2×10^5/mL on a 6-well plate. When the cells reached 100% confluence, changed the differentiation medium and incubated for 10 days. For adipogenic differentiation, the differentiation medium comprised the basic medium with 0.1 μM dexamethasone, 10 μg/mL insulin, 0.5 mM 3-isobutyl-1-methylxanthine (IBMX). Oil red O stain solution was used to show adipocytes. All the regents were provided by the rat BMSC adipogenic differentiation kit (Chem, China; CHEM-200014). For chondrogenic differentiation, the differentiation medium

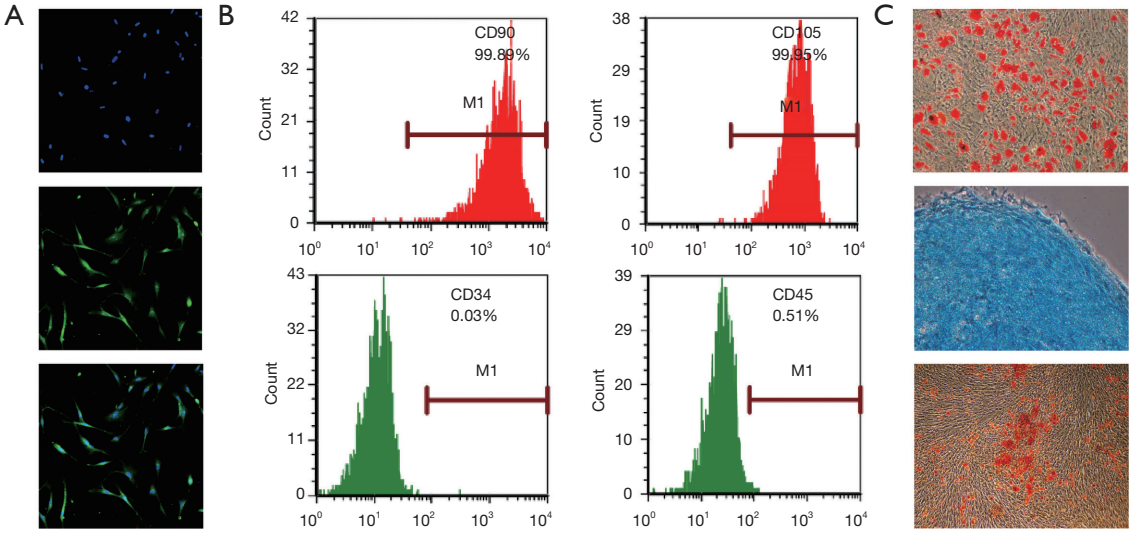

Figure 1 Cell identification. (A) Immunofluorescence staining of S100 for SC identification. Magnification: 20×. (B) Flow cytometry for BMSC identification. (C) BMSCs have the ability to differentiate into adipocytes (oil red O), chondrocytes (Alcian blue) and osteoblasts (Alizarin red). Magnification: 20×. CD, cluster differentiation; SC, Schwann cell; BMSC, bone marrow mesenchymal stem cell.

comprised the basic medium with 0.1 μM dexamethasone, 50 μg/mL ascorbic acid, 6.25 μg/mL insulin, 6.25 μg/mL transferrin. Alcian blue cartilage stain solution was used to show chondrocytes. All the regents were provided by the rat BMSC chondrogenic differentiation kit (Chem, China; CHEM-200015). For osteogenic differentiation, the differentiation medium comprised the basic medium with 1 μM dexamethasone, 50 μg/mL ascorbic acid, 10 mM sodium β-glycerophosphate. Alizarin red stain solution was used to show osteoblasts. All the regents were provided by the rat BMSC osteogenic differentiation kit (Chem, China; CHEM-200016).

Western blot

Western blot was performed as previously described with a minor modification (27). After the cocultures, the BMSCs were lysed with radioimmunoprecipitation supplemented with phenylmethylsulfonyl fluoride. The protein samples were electrophoresed in 10% sodium dodecyl sulfate gel and transferred to polyvinylidene fluoride membranes at 4 ℃. The membranes were cut according to the molecular weight and blocked in 5% skim milk at room temperature for 1 h. Primary antibodies, including anti-collagen VI alpha 2 (Col6a2), anti-intercellular adhesion molecule-1 (ICAM1), anti-Grb2, anti-Col4a2, and anti-P4hb, were used to probe the membranes at 4 ℃ overnight. The membranes were then incubated with secondary antibodies at room temperature for 1 h. The bands were visualized by chemiluminescence.

Statistical analysis

The statistical analysis was performed using SPSS version 15. A one-way analysis of variance with a post-hoc Newman-Keuls multiple comparison test was conducted to identify significant differences among the groups. A P value <0.05 was considered statistically significant.

Results

Cell identification

As *Figure 1A* shows, the SCs were positive for S100. The flow cytometry revealed that the BMSCs were positive for the well-defined BMSC markers of cluster differentiation (CD)90 and CD105, but negative for the hematopoietic surface antigens of CD34 and CD45 (see *Figure 1B*). Further, the BMSCs showed the ability to differentiate into adipocytes, chondrocytes and osteoblasts (see *Figure 1C*). These results indicate that the primary cultures of SCs and BMSCs were successful and could be used for the subsequent proteomics analysis.

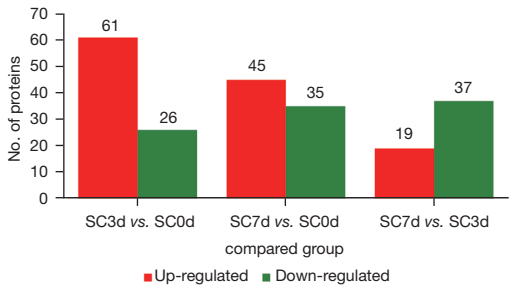

Figure 2 A comparison of the number of the DEPs (up-regulated and down-regulated) in the three groups. SC3d group: the BMSCs were cocultured with SCs for 3 days; SC0d group: the BMSCs were cultured alone; SC7d group: the BMSCs were cocultured with SCs for 7 days. DEPs, differentially expressed proteins; BMSCs, bone marrow mesenchymal stem cells; SCs, Schwann cells.

DEPs identified by proteomic analysis

In total, 6,760 proteins were identified, of which 5,184 were quantified. Trends in changes in protein expression were investigated for the BMSC and SC cocultures for the SC3d and SC7d groups relative to the SC0d group. The differences and similarities in protein differential expression were analyzed. The DEPs were regarded when the difference magnitude among the groups was >1.3-fold, and the result was reproduced twice.

The number of DEPs is shown in *Figure 2*. After comparing the BMSCs cocultured with the SCs for 3 days to the control group (SC3d *vs.* SC0d), 87 DEPs were identified, of which 61 were upregulated and 26 were downregulated (see Table S1). After comparing the BMSCs cocultured with the SCs for 7 days to the control group (SC7d *vs.* SC0d), 80 DEPs were identified, of which 45 were upregulated and 35 were downregulated (see Table S2). After comparing the BMSCs cocultured with the SCs for 7 days to those cocultured for 3 days (SC7d *vs.* SC3d), 56 DEPs were identified, of which 19 were upregulated and 37 were downregulated (see Table S3).

GO analysis

In the GO analysis, the genes or proteins were assessed based on the following three features: biological processes, molecular functions, and cellular components. In relation to the 87 DEPs in the SC3d *vs.* SC0d comparison, the top 10 significantly enriched GO terms were "protein complex involved in cell adhesion", "integrin complex", "extracellular region", "integral component of plasma membrane", "extracellular space", "response to monosaccharide", "integrin-mediated signaling pathway", "extracellular region part", "intrinsic component of plasma membrane", and "response to carbohydrate" (see *Figure 3A*). In relation to the 80 DEPs in the SC7d *vs.* SC0d comparison, the top 10 significantly enriched GO terms were "response to nicotine", "DNA binding, bending", "DNA conformation change", "myoblast proliferation", "meiotic chromosome condensation", "amide binding", "carboxylic acid binding", "DNA packaging complex", "organic acid binding", and "kinetochore organization" (see *Figure 3B*). Finally, in relation to the 56 DEPs in the SC7d *vs.* SC3d comparison, the top 10 significantly enriched GO terms were "procollagen-proline 4-dioxygenase activity", "peptidyl-proline 4-dioxygenase activity", "procollagen-proline dioxygenase activity", "dioxygenase activity", "protein hydroxylation", "peptidyl-proline dioxygenase activity", "oxidoreductase activity, acting on single donors with incorporation of molecular oxygen, incorporation of 2 atoms of oxygen", "oxidoreductase activity, acting on single donors with incorporation of molecular oxygen", "oxidoreductase activity, acting on paired donors, with incorporation or reduction of molecular oxygen, 2-oxoglutarate as one donor, and incorporation of one atom each of oxygen into both donors", and "extracellular space" (see *Figure 3C*).

KEGG pathway analysis

KEGG is a publicly available pathway database that provides biologists with excellent resources to gain a deeper understanding of the biological mechanisms elicited in response to different treatments. According to the KEGG enrichment results for the SC3d *vs.* SC0d comparison, the 10 top significantly enriched KEGG pathways were the "extracellular matrix (ECM)-receptor interaction", "hypertrophic cardiomyopathy (HCM)", "dilated cardiomyopathy", "hematopoietic cell lineage", "microRNAs in cancer", "arrhythmogenic right ventricular cardiomyopathy (ARVC)", "lysosome", "focal adhesion", "phosphatidylinositol-3-kinase (PI3K)-Akt signaling pathway", and "starch and sucrose metabolism" (see *Figure 4A*). According to the KEGG enrichment results for the SC7d *vs.* SC0d comparison, the 10 top significantly enriched KEGG pathways were "HCM", "fatty acid elongation", "ECM-receptor interaction", "fat digestion and absorption", "dilated cardiomyopathy", "ether lipid

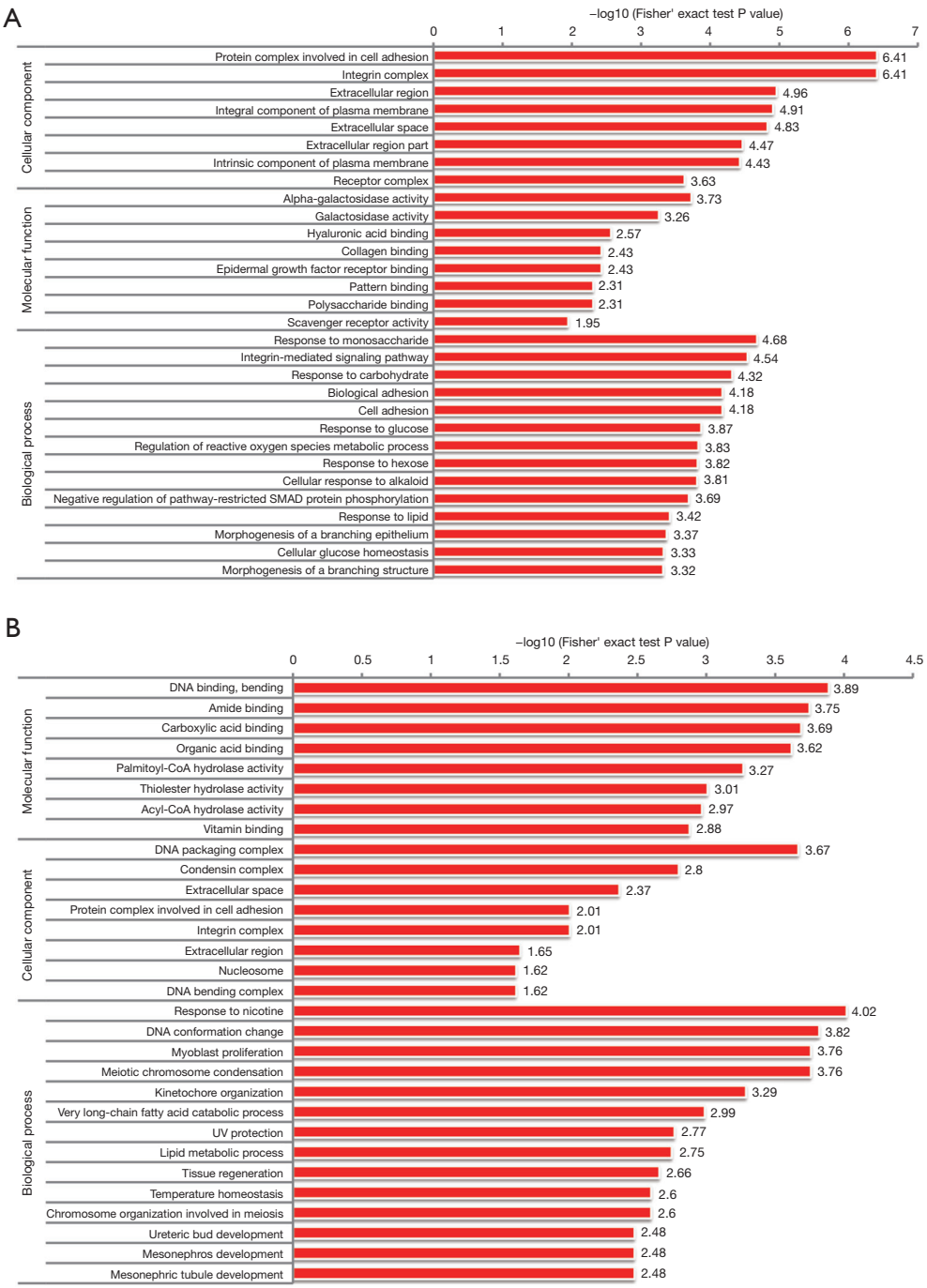

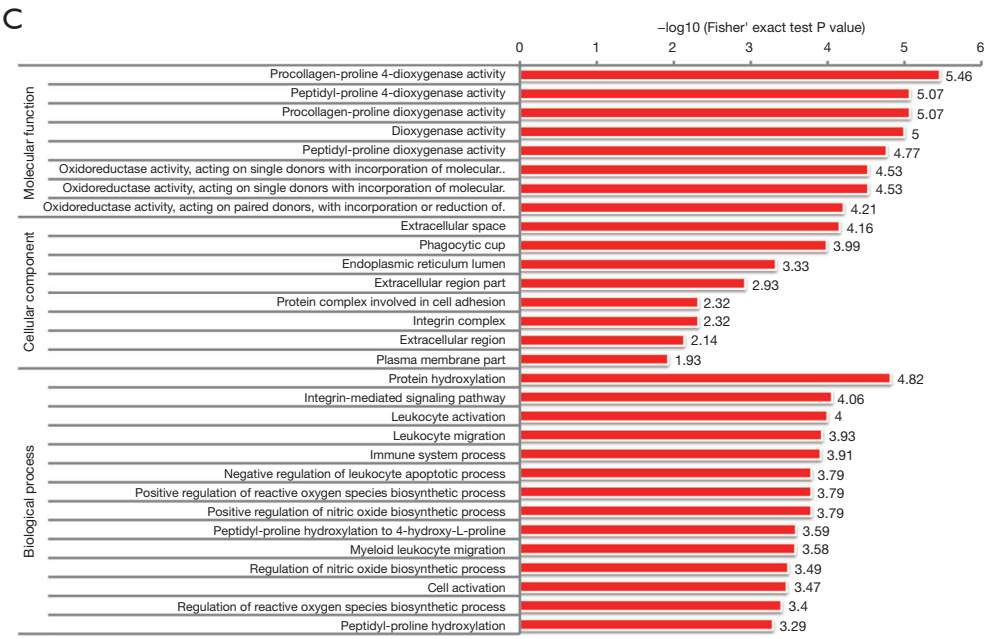

Figure 3 GO enrichment analysis. (A) GO enrichment analysis of the DEPs in the SC3d group *vs.* the SC0d group. (B) GO enrichment analysis of the DEPs in the SC7d group *vs.* the SC0d group. (C) GO enrichment analysis of the DEPs in the SC7d group *vs.* the SC3d group. SC3d group: the BMSCs were cocultured with SCs for 3 days; SC0d group: the BMSCs were cultured alone; SC7d group: the BMSCs were cocultured with SCs for 7 days. UV, ultraviolet; GO, Gene Ontology; DEPs, differentially expressed proteins; BMSCs, bone marrow mesenchymal stem cells; SCs, Schwann cells.

metabolism", "lysosome", and "amyotrophic lateral sclerosis (ALS)" (see *Figure 4B*). According to the KEGG enrichment results for the of SC7d and SC3d comparison, the 10 top significantly enriched KEGG pathways were "amoebiasis", "leishmaniasis", "sulfur metabolism", "staphylococcus aureus infection", "complement and coagulation cascades", "cell adhesion molecules (CAMs)", "tuberculosis", "leukocyte transendothelial migration", "arginine and proline metabolism", and "peroxisome proliferator-activated receptor (PPAR) signaling pathway" (see *Figure 4C*).

PPI network

The PPI network of the DEPs in the SC3d *vs.* SC0d comparison contained 26 nodes and 26 connections (see *Figure 5A*). The PPI network of the DEPs in the SC7d *vs.* SC0d contained 10 nodes and 5 connections (see *Figure 5B*). The PPI network of the DEPs in the SC7d *vs.* SC3d contained 16 nodes and 11 connections (see *Figure 5C*). The top 5 core genes included *Col4a2*, *Col6a2*, *Grb2*, *Icam1*, and *P4hb*. Based on the quantitative data, *Col6a2*, *Grb2*, and *Icam1* were upregulated, while *Col4a2* and *P4hb* were downregulated.

Western blot verification

Western blot was performed to detect the changes in protein levels of the significant DEPs. As *Figure 6* shows, compared to the control group, the protein levels of *Col6a2*, *Icam1* and *Grb2* were significantly upregulated in the coculture group; however, the protein levels of *Col4a2* and *P4hb* were significantly decreased, which is consistent with the results of the quantitative analysis.

Discussion

SCI is a severe condition characterized by high morbidity and disability. Due to its unknown pathological mechanisms, there has been little progress in the management of SCI to date. Our group has a long-standing interest in SCI treatments based on cell transplantation. In previous research, we demonstrated that SCs can both secrete neurotrophic factors to restrict the apoptosis of neurons and

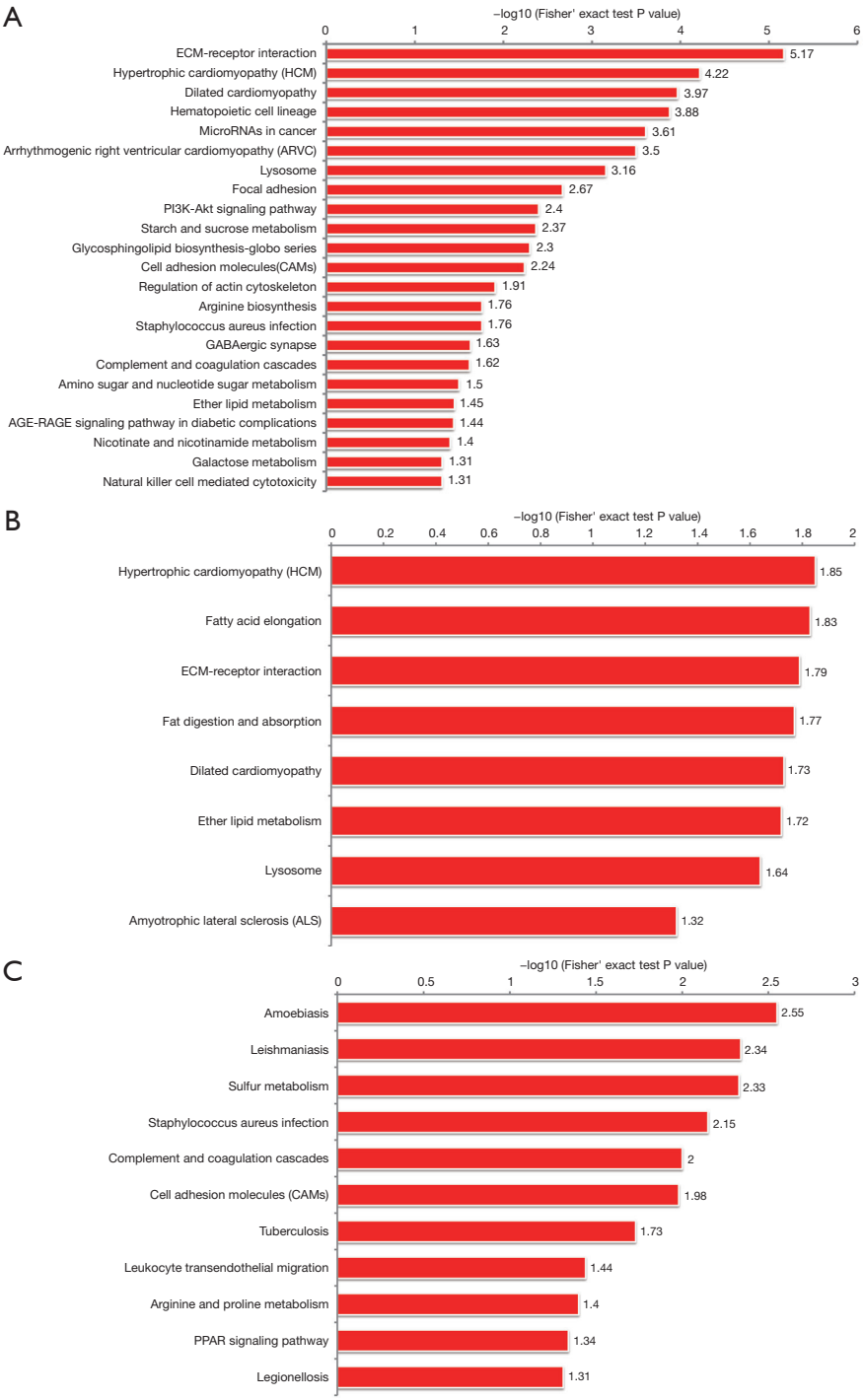

Figure 4 KEGG pathway analysis. (A) KEGG pathway analysis of the DEPs in the SC3d *vs.* SC0d group. (B) KEGG pathway analysis of the DEPs in the SC7d *vs.* SC0d group. (C) KEGG pathway analysis of the DEPs in the SC7d *vs.* SC3d group. SC3d group: the BMSCs were cocultured with SCs for 3 days; SC0d group: the BMSCs were cultured alone; SC7d group: the BMSCs were cocultured with SCs for 7 days. ECM, extracellular matrix; HCM, hypertrophic cardiomyopathy; ARVC, arrhythmogenic right ventricular cardiomyopathy; PI3K, phosphatidylinositol-3-kinase; CAMs, cell adhesion molecules; ALS, amyotrophic lateral sclerosis; PPAR, peroxisome proliferator-activated receptor; KEGG, Kyoto Encyclopedia of Genes and Genomes; DEPs, differentially expressed proteins; BMSCs, bone marrow mesenchymal stem cells; SCs, Schwann cells.

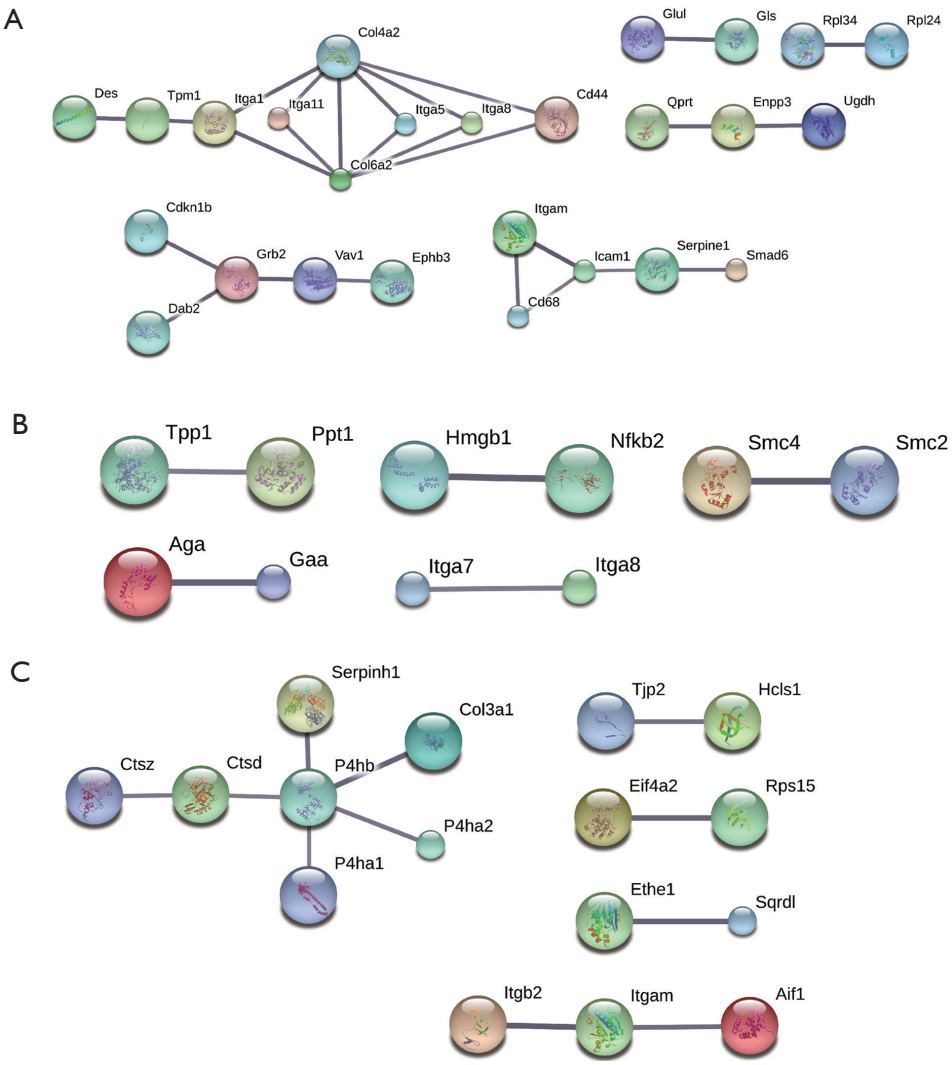

Figure 5 PPI network analysis. (A) PPI network analysis of the DEPs in the SC3d *vs.* the SC0d group. (B) PPI network analysis of the DEPs in the SC7d *vs.* the SC0d group. (C) PPI network analysis of the DEPs in the SC7d *vs.* the SC3d group. SC3d group: the BMSCs were cocultured with SCs for 3 days; SC0d group: the BMSCs were cultured alone; SC7d group: the BMSCs were cocultured with SCs for 7 days. PPI, protein-protein interaction; DEPs, differentially expressed proteins; BMSCs, bone marrow mesenchymal stem cells; SCs, Schwann cells.

induce BMSCs to differentiate into neuron-like cells, which can promote axonal regeneration and functional recovery (21-24). Several studies have shown that miRNA plays an important role in regulating the neuronal differentiation of stem cells, which are involved in regulating Hippo, Wnt and tumor growth factor-beta (TGF-β) signal pathway (28,29). However, the underlying mechanisms of the interaction between these cells remain unclear. Identifying the molecular mechanism of SCI cell graft therapy was a specific aim of the described project. According to the pathological features of SCI, the efficacy and repair mechanism of co-transplantation SCs and BMSCs at different periods after the injury will be further investigated and defined. The goals of the project were to identify targets and cell signaling pathways and to establish a more reliable and effective treatment strategy for cell transplantation. The outcomes of this proposal will shed light on fundamental problems confounding stem cell therapies and pave the way for further SCI research, increasing the likelihood of early rehabilitation and the efficacy of treatments. iTRAQ

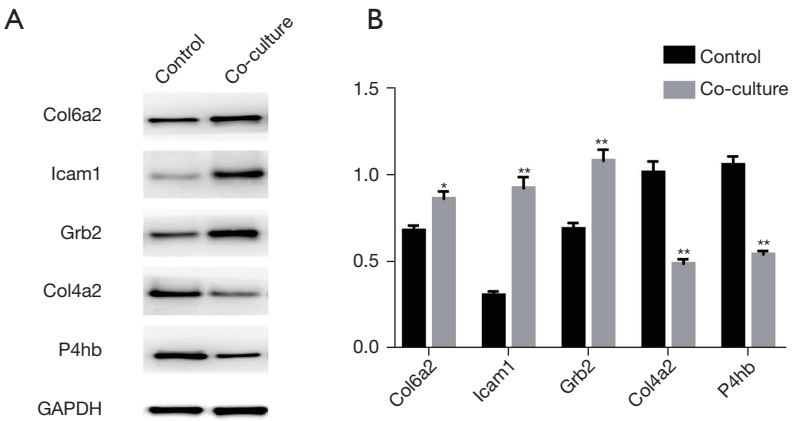

Figure 6 Western blot verification. (A) The expression level of the DEPs. (B) Quantification of the DEPs. *P<0.05, **P<0.01, compared to the control group. DEPs, differentially expressed proteins.

is a method with high throughput, stability, and sensitivity to sample properties, and can be used to evaluate the DEPs quantitatively. iTRAQ technology is developed by AB SCIEX in the US, which has been a new tool for quantitative mass spectrometry and widely used in proteome research. In this study, we used the quantitative iTRAQ proteomics to reveal the proteome profiles and investigate the potential mechanisms.

The GO analysis results for the SC3d *vs.* SC0d comparison show that the "protein complex involved in cell adhesion", "integrin complex", "integral component of plasma membrane", and "integrin-mediated signaling pathway" are significantly enriched pathways. Among the corresponding changes, ICAM1 was upregulated. ICAM1, which is a single-chain cell surface glycoprotein, is a molecule that has significant roles in the inflammatory response and in the recruitment of leukocytes to sites of inflammation (30,31). ICAM1 promotes adhesion at inflammatory sites and regulates the immune response, which is very beneficial in acute SCI. ICAM1 is also believed to be a key factor in inducing angiogenesis, which may ameliorate the ischemia and hypoxia that occur after SCI (32,33).

Integrin and integrin signaling have great significance in axon growth and regeneration in the peripheral nervous system (PNS) and the central nervous system (CNS) (34-36). As a type of transmembrane heterodimeric receptor, integrin may improve bidirectional signaling between the extracellular environment and cells and may have significant roles in cell growth, division, survival, and differentiation (37). Integrin is also important for regulating the coordinated process of leukocyte extravasation into inflammatory sites (38). These three functions are crucial for the repair of SCI. Based on the GO analysis results for the SC7d *vs.* SC3d comparison, most of the significantly enriched terms are related to dioxygenase activity. It has been reported that MSCs regulate the proliferation, activation, and cytotoxicity related to the immune response via dioxygenase (39). Dioxygenase may also reprogram proinflammatory M1-polarized macrophages toward the anti-inflammatory M2-polarized macrophage phenotype, which is essential for maintaining a balanced microenvironment after damage to the CNS (8,39).

The results of the KEGG pathway analysis revealed some terms related to heart disease and the repair of myocardial cell injury, which are applications of MSCs in cardiac research. Given the similar characteristics of myocardial cells and neurons, this result may provide a meaningful research direction for our focus on SCI. Additionally, "lysosome", the "PI3K-Akt signaling pathway", "CAMs", "leukocyte transendothelial migration", and "PPAR signaling pathway" may be crucial in the repair of SCI. Lysosome functionality is an important factor in regulating extracellular vesicle (EV) secretion and contents (40). Exosomes are a subtype of EVs, which are vesicles that are 50–100 nm in diameter and mediate intercellular material transfer. Exosomes carry messenger RNAs, micro RNAs and proteins, which can be detected by various techniques (41,42). From 2012 to 2016, Lopez-Verrilli *et al.* gradually revealed that SC-derived exosomes mediate neuron-glia communication and enhance axonal regeneration in the PNS (43-46). SC-derived exosomes may be involved in a potential mechanism mediating BMSC-stimulated SCI repair. Further, exosomes derived from BMSCs have been

shown to promote angiogenesis and axonal regeneration, suppress glial scar formation and inflammation, and improve functional recovery after SCI (47). Exosomes may also mediate material and signaling exchanges between SCs and BMSCs, but this hypothesis requires further study. The PI3K-Akt signaling pathway was reported to regulate human endometrial stem cell differentiation into motor neurons and have a beneficial effect on ischemia/reperfusion injury after SCI (48,49). SCs may promote BMSC differentiation into neuron-like cells and co-grafting these two types of cells can improve functional recovery after SCI via the PI3K-Akt signaling pathway. As mentioned above, "CAMs" and "leukocyte transendothelial migration" play crucial roles in regulating adhesion at inflammatory sites and in the immune response (30,31). It has been reported that PPAR activation can induce anti-inflammatory and antioxidant effects, provide vascular protection, and inhibit apoptosis in the nervous system; thus, PPAR may be a novel pharmacological target in neuroprotection (50-52).

Conclusions

In summary, the mechanisms that occur during the co-transplantation of BMSCs and SCs are complicated and involve a variety of potential signaling pathways that may be related to regulating the inflammatory response, maintaining a balanced microenvironment, promoting angiogenesis and axonal regeneration, improving neuron-like differentiation, secreting neurotrophic factors, and suppressing glial scar formation. Further verification is required to confirm our hypothesis. These results still need to be verified by further experimental work. We believe that our study may provide potential study targets and novel therapeutic directions.

Acknowledgments

Funding: This work was supported by grants from the National Key R&D Program of China (No. 2019YFA0112100) and the Tianjin Key Medical Discipline (Specialty) Construct Project.

Footnote

Reporting Checklist: The authors have completed the ARRIVE reporting checklist. Available at https://atm.amegroups.com/article/view/10.21037/atm-22-3073/rc

Data Sharing Statement: Available at https://atm.amegroups.com/article/view/10.21037/atm-22-3073/dss

Conflicts of Interest: All authors have completed the ICMJE uniform disclosure form (available at https://atm.amegroups.com/article/view/10.21037/atm-22-3073/coif). The authors have no conflicts of interest to declare.

Ethical Statement: The authors are accountable for all aspects of the work in ensuring that questions related to the accuracy or integrity of any part of the work are appropriately investigated and resolved. Experiments were performed under a project license (No. TMUAMEC2017025) granted by the Tianjin Medical University Ethical Committee, in compliance with the Guide for the Care and Use of Laboratory Animals (NIH Publications, revised 2011).

References

1. Eli I, Lerner DP, Ghogawala Z. Acute Traumatic Spinal Cord Injury. Neurol Clin 2021;39:471-88.
2. Flack JA, Sharma KD, Xie JY. Delving into the recent advancements of spinal cord injury treatment: a review of recent progress. Neural Regen Res 2022;17:283-91.
3. Sharma HS, Winkler T. Assessment of spinal cord pathology following trauma using early changes in the spinal cord evoked potentials: a pharmacological and morphological study in the rat. Muscle Nerve Suppl 2002;11:S83-91.
4. Choo AM, Liu J, Dvorak M, et al. Secondary pathology following contusion, dislocation, and distraction spinal cord injuries. Exp Neurol 2008;212:490-506.
5. Mitchell CS, Lee RH. Pathology dynamics predict spinal cord injury therapeutic success. J Neurotrauma 2008;25:1483-97.
6. Ward RE, Huang W, Kostusiak M, et al. A

characterization of white matter pathology following spinal cord compression injury in the rat. Neuroscience 2014;260:227-39.
7. David S, Kroner A. Repertoire of microglial and macrophage responses after spinal cord injury. Nat Rev Neurosci 2011;12:388-99.
8. Shechter R, Miller O, Yovel G, et al. Recruitment of beneficial M2 macrophages to injured spinal cord is orchestrated by remote brain choroid plexus. Immunity 2013;38:555-69.
9. Hurlbert RJ, Moulton R. Why do you prescribe methylprednisolone for acute spinal cord injury? A Canadian perspective and a position statement. Can J Neurol Sci 2002;29:236-9.
10. Schroeder GD, Kwon BK, Eck JC, et al. Survey of Cervical Spine Research Society members on the use of high-dose steroids for acute spinal cord injuries. Spine (Phila Pa 1976) 2014;39:971-7.
11. Hurlbert RJ, Hamilton MG. Methylprednisolone for acute spinal cord injury: 5-year practice reversal. Can J Neurol Sci 2008;35:41-5.
12. Miekisiak G, Kloc W, Janusz W, et al. Current use of methylprednisolone for acute spinal cord injury in Poland: survey study. Eur J Orthop Surg Traumatol 2014;24 Suppl 1:S269-73.
13. Druschel C, Schaser KD, Schwab JM. Current practice of methylprednisolone administration for acute spinal cord injury in Germany: a national survey. Spine (Phila Pa 1976) 2013;38:E669-77.
14. Khodabandeh Z, Mehrabani D, Dehghani F, et al. Spinal cord injury repair using mesenchymal stem cells derived from bone marrow in mice: A stereological study. Acta Histochem 2021;123:151720.
15. Sykova E, Cizkova D, Kubinova S. Mesenchymal Stem Cells in Treatment of Spinal Cord Injury and Amyotrophic Lateral Sclerosis. Front Cell Dev Biol 2021;9:695900. Erratum in: Front Cell Dev Biol 2021;9:770243.
16. Lin L, Lin H, Bai S, et al. Bone marrow mesenchymal stem cells (BMSCs) improved functional recovery of spinal cord injury partly by promoting axonal regeneration. Neurochem Int 2018;115:80-4.
17. Anderson JD, Johansson HJ, Graham CS, et al. Comprehensive Proteomic Analysis of Mesenchymal Stem Cell Exosomes Reveals Modulation of Angiogenesis via Nuclear Factor-KappaB Signaling. Stem Cells 2016;34:601-13.
18. Zeng X, Zeng YS, Ma YH, et al. Bone marrow mesenchymal stem cells in a three-dimensional gelatin sponge scaffold attenuate inflammation, promote angiogenesis, and reduce cavity formation in experimental spinal cord injury. Cell Transplant 2011;20:1881-99.
19. Kim GU, Sung SE, Kang KK, et al. Therapeutic Potential of Mesenchymal Stem Cells (MSCs) and MSC-Derived Extracellular Vesicles for the Treatment of Spinal Cord Injury. Int J Mol Sci 2021;22:13672.
20. Stratton JA, Shah PT. Macrophage polarization in nerve injury: do Schwann cells play a role? Neural Regen Res 2016;11:53-7.
21. Feng SQ, Kong XH, Guo SF, et al. Treatment of spinal cord injury with co-grafts of genetically modified Schwann cells and fetal spinal cord cell suspension in the rat. Neurotox Res 2005;7:169-77.
22. Ban DX, Kong XH, Feng SQ, et al. Intraspinal cord graft of autologous activated Schwann cells efficiently promotes axonal regeneration and functional recovery after rat's spinal cord injury. Brain Res 2009;1256:149-61.
23. Ban DX, Ning GZ, Feng SQ, et al. Combination of activated Schwann cells with bone mesenchymal stem cells: the best cell strategy for repair after spinal cord injury in rats. Regen Med 2011;6:707-20.
24. Zhou XH, Ning GZ, Feng SQ, et al. Transplantation of autologous activated Schwann cells in the treatment of spinal cord injury: six cases, more than five years of follow-up. Cell Transplant 2012;21 Suppl 1:S39-47.
25. Zhou XH, Lin W, Ren YM, et al. Comparison of DNA Methylation in Schwann Cells before and after Peripheral Nerve Injury in Rats. Biomed Res Int 2017;2017:5393268.
26. Spanos C, Moore JB. Sample Preparation Approaches for iTRAQ Labeling and Quantitative Proteomic Analyses in Systems Biology. Methods Mol Biol 2016;1394:15-24.
27. Pan D, Li Y, Yang F, et al. Increasing toll-like receptor 2 on astrocytes induced by Schwann cell-derived exosomes promotes recovery by inhibiting CSPGs deposition after spinal cord injury. J Neuroinflammation 2021;18:172.
28. Wei ZJ, Fan BY, Liu Y, et al. MicroRNA changes of bone marrow-derived mesenchymal stem cells differentiated into neuronal-like cells by Schwann cell-conditioned medium. Neural Regen Res 2019;14:1462-9.
29. Channakkar AS, Singh T, Pattnaik B, et al. MiRNA-137-mediated modulation of mitochondrial dynamics regulates human neural stem cell fate. Stem Cells 2020;38:683-97.
30. Liu J, Liu Z, Liu G, et al. Spinal cord injury and its underlying mechanism in rats with temporal lobe epilepsy. Exp Ther Med 2020;19:2103-12.
31. Singh M, Thakur M, Mishra M, et al. Gene regulation of intracellular adhesion molecule-1 (ICAM-1): A molecule

with multiple functions. Immunol Lett 2021;240:123-36.
32. Wang L, Yao Y, He R, et al. Methane ameliorates spinal cord ischemia-reperfusion injury in rats: Antioxidant, anti-inflammatory and anti-apoptotic activity mediated by Nrf2 activation. Free Radic Biol Med 2017;103:69-86.
33. Günday M, Saritaş ZK, Demirel HH, et al. Does Anzer Propolis Have a Protective Effect on Rabbit Spinal Cord Ischemia/Reperfusion Injury? Braz J Cardiovasc Surg 2022;37:65-73.
34. Ikeshima-Kataoka H, Sugimoto C, Tsubokawa T. Integrin Signaling in the Central Nervous System in Animals and Human Brain Diseases. Int J Mol Sci 2022;23:1435.
35. Eva R, Fawcett J. Integrin signalling and traffic during axon growth and regeneration. Curr Opin Neurobiol 2014;27:179-85.
36. Sekine Y, Kannan R, Wang X, et al. Rabphilin3A reduces integrin-dependent growth cone signaling to restrict axon regeneration after trauma. Exp Neurol 2022;353:114070.
37. Xiong J, Yan L, Zou C, et al. Integrins regulate stemness in solid tumor: an emerging therapeutic target. J Hematol Oncol 2021;14:177.
38. Sun H, Hu L, Fan Z. β2 integrin activation and signal transduction in leukocyte recruitment. Am J Physiol Cell Physiol 2021;321:C308-16.
39. Zheng G, Ge M, Qiu G, et al. Mesenchymal Stromal Cells Affect Disease Outcomes via Macrophage Polarization. Stem Cells Int 2015;2015:989473.
40. Eitan E, Suire C, Zhang S, et al. Impact of lysosome status on extracellular vesicle content and release. Ageing Res Rev 2016;32:65-74.
41. Jan AT, Rahman S, Khan S, et al. Biology, Pathophysiological Role, and Clinical Implications of Exosomes: A Critical Appraisal. Cells 2019;8:99.
42. Dilsiz N. Hallmarks of exosomes. Future Sci OA 2022;8:FSO764.
43. Lopez-Verrilli MA, Court FA. Transfer of vesicles from schwann cells to axons: a novel mechanism of communication in the peripheral nervous system. Front Physiol 2012;3:205.
44. Lopez-Verrilli MA, Picou F, Court FA. Schwann cell-derived exosomes enhance axonal regeneration in the peripheral nervous system. Glia 2013;61:1795-806.
45. López-Leal R, Alvarez J, Court FA. Origin of axonal proteins: Is the axon-schwann cell unit a functional syncytium? Cytoskeleton (Hoboken) 2016;73:629-39.
46. Lopez-Leal R, Court FA. Schwann Cell Exosomes Mediate Neuron-Glia Communication and Enhance Axonal Regeneration. Cell Mol Neurobiol 2016;36:429-36.
47. Liu W, Wang Y, Gong F, et al. Exosomes Derived from Bone Mesenchymal Stem Cells Repair Traumatic Spinal Cord Injury by Suppressing the Activation of A1 Neurotoxic Reactive Astrocytes. J Neurotrauma 2019;36:469-84.
48. Ebrahimi-Barough S, Hoveizi E, Yazdankhah M, et al. Inhibitor of PI3K/Akt Signaling Pathway Small Molecule Promotes Motor Neuron Differentiation of Human Endometrial Stem Cells Cultured on Electrospun Biocomposite Polycaprolactone/Collagen Scaffolds. Mol Neurobiol 2017;54:2547-54.
49. Zhang F, Ru N, Shang ZH, et al. Daidzein ameliorates spinal cord ischemia/reperfusion injury-induced neurological function deficits in Sprague-Dawley rats through PI3K/Akt signaling pathway. Exp Ther Med 2017;14:4878-86.
50. Wnuk A, Kajta M. Steroid and Xenobiotic Receptor Signalling in Apoptosis and Autophagy of the Nervous System. Int J Mol Sci 2017;18:2394.
51. Mannan A, Garg N, Singh TG, et al. Peroxisome Proliferator-Activated Receptor-Gamma (PPAR-ɣ): Molecular Effects and Its Importance as a Novel Therapeutic Target for Cerebral Ischemic Injury. Neurochem Res 2021;46:2800-31.
52. Toobian D, Ghosh P, Katkar GD. Parsing the Role of PPARs in Macrophage Processes. Front Immunol 2021;12:783780.

(English Language Editor: L. Huleatt)

Cite this article as: Ding H, Li A, Sun C, Zhang J, Shang J, Tang H, Li J, Wang M, Kong X, Wei Z, Feng S. Quantitative iTRAQ proteomics reveal the proteome profiles of bone marrow mesenchymal stem cells after cocultures with Schwann cells *in vitro*. Ann Transl Med 2022;10(18):962. doi: 10.21037/atm-22-3073

Supplementary

Table S1 DEPs in SC3d *vs.* SC0d group

Protein description	SC3d *vs.* SC0d ratio	Regulated type	P value	Gene name
Glutaminase kidney isoform, mitochondrial	0.71100	Down	0.04765	*Gls*
60S ribosomal protein L34	0.44400	Down	0.04185	*Rpl34*
Protein Itga8	0.44000	Down	0.04215	*Itga8*
Plexin domain containing 2	0.73467	Down	0.04335	*Plxdc2*
Eph receptor B3 (predicted)	0.69800	Down	0.01831	*Ephb3*
Protein Diras2	0.45800	Down	0.00900	*Diras2*
Protein Susd5	0.57533	Down	0.01300	*Susd5*
Protein RGD1559896	0.71967	Down	0.04529	*RGD1559896*
Condensin complex subunit 2	0.54250	Down	0.02576	*Ncaph*
Protein Itga11	0.56300	Down	0.04515	*Itga11*
Protein Afap1l2	0.51900	Down	0.03572	*Afap1l2*
Protein Col4a2	0.67600	Down	0.00375	*Col4a2*
Phospholipid phosphatase 1	0.58833	Down	0.00969	*Plpp1*
Matrix Gla protein	0.54667	Down	0.03961	*Mgp*
Stathmin	0.69700	Down	0.04281	*Stmn1*
Integrin alpha-1	0.54967	Down	0.03478	*Itga1*
Stathmin-2	0.74667	Down	0.01517	*Stmn2*
Myristoylated alanine-rich C-kinase substrate	0.62767	Down	0.04282	*Marcks*
Transporter	0.26800	Down	0.00953	*Slc6a6*
Methionine aminopeptidase 2	0.70000	Down	0.00082	*Metap2*
Thymosin beta-4	0.68800	Down	0.03182	*Tmsb4x*
60S ribosomal protein L24	0.44267	Down	0.02973	*Rpl24*
Chondroitin sulfate proteoglycan 4	0.67333	Down	0.00128	*Cspg4*
Phosphoserine phosphatase	0.56967	Down	0.04604	*Psph*
Integrin beta-like protein 1	0.70033	Down	0.01679	*Itgbl1*
Fibulin-5	0.45667	Down	0.03592	*Fbln5*
Tropomyosin 1, alpha, isoform CRA_p	1.65967	Up	0.01491	*Tpm1*
Integrin alpha 5 (mapped)	1.37267	Up	0.04161	*Itga5*
Protein Nectin2	1.34850	Up	0.04349	*Nectin2*
Prkr interacting protein 1 (IL11 inducible)	1.48150	Up	0.04710	*Prkrip1*
Coactosin-like protein	2.90233	Up	0.04030	*Cotl1*
WD repeat-containing protein 91	1.48450	Up	0.01765	*Wdr91*
Niban-like protein 1	1.48400	Up	0.04661	*Fam129b*
Mothers against decapentaplegic homolog	1.34350	Up	0.02835	*Smad6*
Protein Uap1	2.80267	Up	0.03049	*Uap1*
Protein Tsen15	1.48933	Up	0.02722	*Tsen15*
Cytokine receptor-like factor 1 (predicted)	1.75767	Up	0.02096	*Crlf1*
Protein Gla	1.35700	Up	0.00108	*Gla*
HD domain containing 2 (predicted), isoform CRA_b	1.78167	Up	0.00812	*Hddc2*
Protein Cenpv	1.31100	Up	0.00781	*Cenpv*
Procollagen, type VI, alpha 2, isoform CRA_a	1.37833	Up	0.03715	*Col6a2*
Lipid phosphate phosphatase-related protein type 2	22.67950	Up	0.02019	*Prg4*
Integrin alpha M	2.49167	Up	0.02136	*Itgam*
Proto-oncogene vav	2.08750	Up	0.00029	*Vav1*
Protein Znrf2	1.37233	Up	0.04480	*Znrf2*
Cyclin dependent kinase inhibitor	1.37900	Up	0.00609	*Cdkn1b*
Gremlin-1	1.49533	Up	0.02414	*Grem1*
Equilibrative nucleoside transporter 1	1.35100	Up	0.00267	*Slc29a1*
UDP-glucose 6-dehydrogenase	1.95333	Up	0.01789	*Ugdh*
Disabled homolog 2	1.83233	Up	0.04134	*Dab2*
Gamma-enolase	1.76000	Up	0.04039	*Eno2*
Superoxide dismutase [Mn], mitochondrial	2.82067	Up	0.02199	*Sod2*
Glutamine synthetase	1.34267	Up	0.02053	*Glul*
Lysophosphatidylcholine acyltransferase 2	1.57600	Up	0.01852	*Lpcat2*
Corticosteroid 11-beta-dehydrogenase isozyme 1	4.55200	Up	0.03443	*Hsd11b1*
Plasminogen activator inhibitor 1	1.85067	Up	0.03262	*Serpine1*
CD44 antigen	1.31333	Up	0.03845	*Cd44*
Hexokinase	3.93033	Up	0.02873	*Hk3*
Palmitoyl-protein thioesterase 1	1.70800	Up	0.00725	*Ppt1*
Desmin	1.54200	Up	0.03324	*Des*
Cellular retinoic acid-binding protein 2	2.53800	Up	0.01251	*Crabp2*
Growth factor receptor-bound protein 2	1.42300	Up	0.04777	*Grb2*
Cytochrome c oxidase subunit 7C, mitochondrial	1.58667	Up	0.02097	*Cox7c*
Ectonucleotide pyrophosphatase/ phosphodiesterase family member 3	3.15700	Up	0.04419	*Enpp3*
Intercellular adhesion molecule 1	2.87400	Up	0.03069	*Icam1*
Cd68 molecule	5.77267	Up	0.04400	*Cd68*
Leukocyte elastase inhibitor A	1.77533	Up	0.01268	*Serpinb1a*
Paraspeckle component 1	1.32267	Up	0.02228	*Pspc1*
Protein FAM162A	2.25400	Up	0.03564	*Fam162a*
GTP-binding protein SAR1b	1.35400	Up	0.02242	*Sar1b*
Nicotinate-nucleotide pyrophosphorylase [carboxylating]	1.95367	Up	0.04248	*Qprt*
Solute carrier family 12 member 7	1.38633	Up	0.01164	*Slc12a7*
Sorting nexin-3	1.37367	Up	0.03758	*Snx3*
Cytochrome b ascorbate-dependent protein 3	1.41033	Up	0.00999	*Cyb561a3*
Protein Stom	2.34567	Up	0.03631	*Stom*
Alpha-N-acetylgalactosaminidase	1.56200	Up	0.04051	*Naga*
Protective protein for beta-galactosidase	1.79567	Up	0.01784	*Ctsa*
N(G),N(G)-dimethylarginine dimethylaminohydrolase 2	1.43833	Up	0.01664	*Ddah2*
Dolichyl-phosphate (UDP-N-acetylglucosamine) N-acetylglucosaminephosphotrans	1.48767	Up	0.01989	*Dpagt1*
Lactate dehydrogenase D, isoform CRA_d	1.45450	Up	0.01404	*Ldhd*
Optineurin	1.30067	Up	0.03192	*Optn*
Multidrug resistance protein 1a	1.43867	Up	0.00342	*Abcb1a*
Legumain	2.00133	Up	0.04686	*Lgmn*
Cathepsin Z	5.19367	Up	0.04529	*Ctsz*
Guanine deaminase	3.01567	Up	0.04549	*Gda*
Protein Tgm2	2.73533	Up	0.02991	*Tgm2*
Glutathione S-transferase Mu 5	1.43133	Up	0.03360	*Gstm5*

SC3d group: the BMSCs were cocultured with SCs for 3 days; SC0d group: the BMSCs were cultured alone. DEPs, differentially expressed proteins; BMSCs, bone marrow mesenchymal stem cells; SCs, Schwann cells.

https://dx.doi.org/10.21037/atm-22-3073

Table S2 DEPs in SC7d *vs.* SC0d group

Protein description	SC7d *vs.* SC0d ratio	Regulated type	P value	Gene name
DNA helicase	0.64433	Down	0.00035	*Mcm6*
Septin-8	0.75900	Down	0.01255	*Sept8*
Protein Ewsr1	0.74200	Down	0.01354	*Ewsr1*
Protein Itga8	0.58800	Down	0.01627	*Itga8*
Leprecan-like 2 (predicted), isoform CRA_b	0.66333	Down	0.00672	*P3h3*
Histone H1.5	0.66367	Down	0.02966	*Hist1h1b*
Protein Diras2	0.62133	Down	0.02124	*Diras2*
Protein Susd5	0.66233	Down	0.00544	*Susd5*
Structural maintenance of chromosomes protein	0.76100	Down	0.01213	*Smc2*
Structural maintenance of chromosomes protein	0.75333	Down	0.00653	*Smc4*
Protein Cdh11	0.66233	Down	0.02628	*Cdh11*
Muscleblind-like protein 2	0.65867	Down	0.02806	*Mbnl2*
Histone H2B	0.73900	Down	0.00557	*Hist1h2bk*
Phospholipid phosphatase 1	0.43533	Down	0.01835	*Plpp1*
Fatty acid synthase	0.74567	Down	0.03194	*Fasn*
Stathmin	0.51767	Down	0.01136	*Stmn1*
Stathmin-2	0.55833	Down	0.00270	*Stmn2*
Myristoylated alanine-rich C-kinase substrate	0.59433	Down	0.02868	*Marcks*
Methionine aminopeptidase 2	0.73100	Down	0.04900	*Metap2*
Alanine-tRNA ligase, cytoplasmic	0.73233	Down	0.03662	*Aars*
High mobility group protein B2	0.49400	Down	0.01549	*Hmgb2*
Cellular nucleic acid-binding protein	0.75700	Down	0.02939	*Cnbp*
High mobility group protein B1	0.67900	Down	0.03216	*Hmgb1*
Cysteine-rich protein 1	0.44233	Down	0.01418	*Crip1*
Eukaryotic elongation factor 2 kinase	0.72167	Down	0.03912	*Eef2k*
LIM domain-containing protein 2	0.63933	Down	0.02997	*Limd2*
Phosphoserine phosphatase	0.62200	Down	0.02677	*Psph*
Procollagen-lysine, 2-oxoglutarate 5-dioxygenase 1	0.69833	Down	0.03888	*Plod1*
Eukaryotic translation initiation factor 1A	0.74600	Down	0.00742	*Eif1a*
Amino acid transporter	0.70567	Down	0.03963	*Slc1a4*
Heterogeneous nuclear ribonucleoprotein F	0.76667	Down	0.01818	*Hnrnpf*
Dihydrofolate reductase	0.51233	Down	0.02501	*Dhfr*
Caspase	0.70267	Down	0.03594	*Casp12*
RNA-binding protein 3	0.49867	Down	0.01137	*Rbm3*
Fibulin-5	0.56733	Down	0.03576	*Fbln5*
Tropomyosin 1, alpha, isoform CRA_p	1.58200	Up	0.04437	*Tpm1*
Protein Sqrdl	1.42967	Up	0.03004	*Sqrdl*
Protein Tcf25	1.39533	Up	0.04097	*Tcf25*
Fibronectin type III domain containing 3a (predicted), isoform CRA_a	1.30167	Up	0.04862	*Fndc3a*
Cytokine receptor-like factor 1 (predicted)	2.43633	Up	0.01100	*Crlf1*
Protein Isca2	1.42500	Up	0.02853	*Isca2*
Protein Samd4b	1.37750	Up	0.03772	*Samd4b*
Protein Tns3	1.32400	Up	0.01805	*Tns3*
Protein Bag4	1.31900	Up	0.00740	*Bag4*
Protein Slc27a4	1.34433	Up	0.03870	*Slc27a4*
Protein Sowahc	1.40800	Up	0.02055	*Sowahc*
Guanine nucleotide-binding protein subunit beta-4	1.36900	Up	0.03348	*Gnb4*
Acyl-CoA thioesterase 2	1.30767	Up	0.00991	*Acot2*
Anionic trypsin-1	1.36967	Up	0.04309	*Prss1*
Glutathione peroxidase	1.31567	Up	0.02552	*Gpx1*
Catalase	1.32000	Up	0.01704	*Cat*
Lysophosphatidylcholine acyltransferase 2	1.30967	Up	0.00413	*Lpcat2*
Hemoglobin subunit beta-1	3.30833	Up	0.02940	*Hbb*
Interleukin 1 receptor antagonist, isoform CRA_c	1.99550	Up	0.00490	*Il1rn*
N(4)-(Beta-N-acetylglucosaminyl)-L-asparaginase	1.93600	Up	0.00504	*Aga*
Tricarboxylate transport protein, mitochondrial	1.32767	Up	0.01994	*Slc25a1*
Syndecan-4	1.35200	Up	0.02499	*Sdc4*
Palmitoyl-protein thioesterase 1	1.37067	Up	0.01734	*Ppt1*
Cellular retinoic acid-binding protein 2	2.67167	Up	0.04130	*Crabp2*
ES1 protein homolog, mitochondrial	1.42033	Up	0.00328	*P56571*
Myotrophin	1.39833	Up	0.01201	*Mtpn*
D-2-hydroxyglutarate dehydrogenase, mitochondrial	1.66700	Up	0.04224	*D2hgdh*
ATP synthase F(0) complex subunit C1, mitochondrial	1.57667	Up	0.00117	*Atp5g1*
Testin	1.52800	Up	0.01224	*Tes*
GTP-binding protein SAR1b	1.39833	Up	0.04618	*Sar1b*
Eukaryotic initiation factor 4A-II	1.48100	Up	0.01698	*Eif4a2*
High-mobility group nucleosome binding domain 1	1.57300	Up	0.02981	*LOC100911295*
Nuclear factor of kappa light polypeptide gene enhancer in B-cells 2, p49/p100	1.44767	Up	0.03563	*Nfkb2*
Coenzyme A synthase	1.45367	Up	0.03440	*Coasy*
Integrin alpha-7	1.65333	Up	0.01732	*Itga7*
Podoplanin	1.65200	Up	0.03801	*Pdpn*
E3 ubiquitin-protein ligase RNF181	1.54700	Up	0.01510	*Rnf181*
N(G),N(G)-dimethylarginine dimethylaminohydrolase 2	1.41000	Up	0.00046	*Ddah2*
Glucosidase, alpha, acid, isoform CRA_a	1.33300	Up	0.03159	*Gaa*
Protein FAM198B	1.30200	Up	0.02176	*Fam198b*
Protein Serpinb6	1.30833	Up	0.04043	*Serpinb6*
Plectin	1.31933	Up	0.03953	*Plec*
Tripeptidyl-peptidase 1	1.35733	Up	0.02985	*Tpp1*
Neurogenic locus notch homolog protein 2	1.37433	Up	0.04579	*Notch2*
Vesicle-associated membrane protein-associated protein B	1.31700	Up	0.04825	*Vapb*

SC7d group: the BMSCs were cocultured with SCs for 7 days; SC0d group: the BMSCs were cultured alone. DEPs, differentially expressed proteins; BMSCs, bone marrow mesenchymal stem cells; SCs, Schwann cells.

https://dx.doi.org/10.21037/atm-22-3073

Table S3 DEPs in SC7d *vs.* SC3d group

Protein description	SC7d *vs.* SC3d ratio	Regulated type	P value	Gene name
Protein P4ha2	0.50833	Down	0.04720	*P4ha2*
Protein Siglec1	0.51467	Down	0.02247	*Siglec1*
Neutrophil cytosol factor 2	0.39350	Down	0.04285	*Ncf2*
Coactosin-like protein	0.33667	Down	0.03072	*Cotl1*
Sorting nexin-5	0.75733	Down	0.04428	*Snx5*
Integrin beta	0.33600	Down	0.02822	*Itgb2*
Histone H1.5	0.60300	Down	0.02327	*Hist1h1b*
Asparagine-linked glycosylation 9 homolog (yeast, alpha 1,2 mannosyltransferase)	0.64767	Down	0.00322	*Alg9*
HD domain containing 2 (Predicted), isoform CRA_b	0.52533	Down	0.03018	*Hddc2*
Protein Rufy1	0.76600	Down	0.01504	*Rufy1*
Lipid phosphate phosphatase-related protein type 2	0.05500	Down	0.01129	*Prg4*
O-acyltransferase	0.64400	Down	0.04123	*Soat1*
Protein Cetn3	0.76033	Down	0.01911	*Cetn3*
Integrin alpha M	0.39633	Down	0.04183	*Itgam*
Histone H2B	0.73433	Down	0.03059	*Hist1h2bk*
Protein disulfide-isomerase	0.67767	Down	0.04143	*P4hb*
Superoxide dismutase [Mn], mitochondrial	0.55533	Down	0.01577	*Sod2*
Collagen alpha-1(III) chain	0.41067	Down	0.02311	*Col3a1*
Fcer1g protein	0.24900	Down	0.03637	*Fcer1g*
Cathepsin D	0.50833	Down	0.03169	*Ctsd*
Serpin H1	0.26500	Down	0.02638	*Serpinh1*
Alcohol dehydrogenase [NADP(+)]	0.74600	Down	0.03223	*Akr1a1*
Prolyl 4-hydroxylase subunit alpha-1	0.73567	Down	0.04625	*P4ha1*
Allograft inflammatory factor 1	0.17033	Down	0.00104	*Aif1*
40S ribosomal protein S15	0.76100	Down	0.00555	*Rps15*
Fatty acid-binding protein, adipocyte	0.14050	Down	0.01796	*Fabp4*
Proteasome subunit beta type-10	0.66967	Down	0.04877	*Psmb10*
Glutamine--fructose-6-phosphate aminotransferase [isomerizing] 2	0.59250	Down	0.04202	*Gfpt2*
Protein Arhgdib	0.24767	Down	0.02537	*Arhgdib*
Protein Lcp1	0.22267	Down	0.02696	*Lcp1*
Procollagen-lysine, 2-oxoglutarate 5-dioxygenase 1	0.60367	Down	0.03539	*Plod1*
Alpha-N-acetylgalactosaminidase	0.74233	Down	0.04984	*Naga*
Peptidyl-prolyl cis-trans isomerase FKBP9	0.74200	Down	0.04423	*Fkbp9*
Hematopoietic cell specific Lyn substrate 1	0.34200	Down	0.03622	*Hcls1*
N-myc downstream regulated gene 2, isoform CRA_b	0.71650	Down	0.02072	*Ndrg2*
Dihydrofolate reductase	0.60900	Down	0.00803	*Dhfr*
Cathepsin Z	0.21667	Down	0.04974	*Ctsz*
Protein Sqrdl	1.44067	Up	0.04138	*Sqrdl*
Ethylmalonic encephalopathy 1	1.32433	Up	0.04756	*Ethe1*
Protein Zc2hc1a	1.35133	Up	0.03204	*Zc2hc1a*
Protein Isca2	1.31900	Up	0.00986	*Isca2*
Protein Dysf	1.38967	Up	0.02960	*Dysf*
Protein Arhgef5	1.54733	Up	0.04640	*Arhgef5*
Sorbin and SH3 domain-containing protein 1	1.44400	Up	0.01781	*Sorbs1*
Actin filament-associated protein 1	1.30867	Up	0.01104	*Afap1*
Carboxypeptidase E	1.49400	Up	0.01201	*Cpe*
PDZ and LIM domain protein 1	1.34967	Up	0.03252	*Pdlim1*
Fibroblast growth factor 1	1.46867	Up	0.02477	*Fgf1*
Visinin-like protein 1	2.15033	Up	0.01830	*Vsnl1*
Calponin-1	1.48567	Up	0.02286	*Cnn1*
Lysophosphatidylcholine acyltransferase 1	1.42900	Up	0.01995	*Lpcat1*
Protein Tjp2	1.40733	Up	0.01788	*Tjp2*
Probable 2-oxoglutarate dehydrogenase E1 component DHKTD1, mitochondrial	1.32150	Up	0.02809	*Dhtkd1*
Eukaryotic initiation factor 4A-II	1.35433	Up	0.02116	*Eif4a2*
Protein Serpinb9	1.89467	Up	0.04737	*Serpinb9*
Calcium uptake protein 1, mitochondrial	1.52450	Up	0.01470	*Micu1*

SC7d group: the BMSCs were cocultured with SCs for 7 days; SC3d group: the BMSCs were cocultured with SCs for 3 days. DEPs, differentially expressed proteins; BMSCs, bone marrow mesenchymal stem cells; SCs, Schwann cells.

https://dx.doi.org/10.21037/atm-22-3073